

Radiofrequency Ablation of Porcine Adrenal Glands: Interactive Guidance on a High-Field Interventional MR Scanner

S. G. Nour^{1,2}, S. Paul¹, J. O. Heidenreich¹, J. J. Derakhshan², F. Abdulkarim³, M. E. Joseph⁴, M. A. Griswold¹, and J. L. Duerk^{1,2}

¹Radiology, University Hospitals of Cleveland, Cleveland, OH, United States, ²Biomedical Engineering, Case Western Reserve University, Cleveland, OH, United States, ³Pathology, University Hospitals of Cleveland, Cleveland, OH, United States, ⁴Cardiology Research Lab, University Hospitals of Cleveland, Cleveland, OH, United States

Objectives: Percutaneous RFA procedures performed under the guidance and monitoring of low-field MRI have been reported in human subjects and animal models. MRI guidance has shown a particular value when attempting targets within regions of complex anatomy. The aim of this work is to: (1) evaluate the utility of a new state-of-the-art open bore high-field MRI scanner for interventional use; (2) test the feasibility of the first (to our knowledge) adrenal gland RF ablation performed entirely within an MRI suite; and to (3) record the physiological and biochemical changes associated with adrenal ablation.

Material and Methods: 15 MR-guided RFA procedures were performed in the adrenal glands of 13 pigs under IV anesthesia, using a protocol approved by the IACUC. All procedures were performed on a new 1.5 T open bore MR scanner (Espree, Siemens, Germany) supplemented with in-room monitor. The system possesses a short (125 cm) and wide (70 cm) bore designed to allow MR guided interventions. A 3-cm tip 17G MR-compatible titanium RF-electrode (Radionics Inc, Burlington, MA) was introduced under tri-plane real-time MR guidance using True-FISP sequence (TR/TE/FA/NSA: 4/2/60°/3) (Fig. 1). Standard, non-cool tip ablations were conducted at $90 \pm 2^\circ\text{C}$ for 10 minutes using a 200-W RF generator (RFG-3C: Radionics Inc., Burlington, MA) operating at 500 kHz. RF current, power, and impedance were continuously recorded. Continuous intraarterial blood pressure monitoring as well as baseline, immediate and 1-hour post-ablation central venous (IVC) catecholamine, glucose, cortisol, and ACTH levels were obtained ($n=9$).

Post-ablation scans consisted of True-FISP (TR/TE/FA/NSA: 7/3.5/70/3), TSE T2 (TR/TE/NSA/ETL: 7470/102/10/27), TSE STIR (TR/TE/TI/ETL: 5060/77/150/7), and pre- and post-gadolinium SE T1-weighted (TR/TE/FA/NSA: 600/14/90/3) images. Acute animal models ($n=5$) were immediately sacrificed and chronic models ($n=10$) were sacrificed after 2-week follow-up MR scans. Tissue specimens were obtained for pathological examination. Data analysis consisted of evaluation of the ease of access to the magnet isocenter, target and interventional device visualization, median electrode placement time, size and MRI signal characteristics of ablation zones, mean RF current and impedance, and variation in blood pressure and biochemical marker levels.

Results: Access to the magnet's isocenter (coincident with location of the adrenal glands) during MR guided electrode placement was feasible in all procedures. High SNR images were acquired in a time-efficient manner (2.3 s/frame) during device guidance. This facilitated reliable real-time visualization of both the target anatomy and the interventional device. The median electrode placement time was 4 minutes. Adrenal ablation zones demonstrated MRI signal (Fig. 2) and enhancement patterns consistent with previous reports in other organs: i.e., hypointense on all pulse sequences with surrounding hyperintense rim on T2WI that enhances on post-gadolinium scans. Histopathological analysis confirmed tissue necrosis (Fig. 2). The mean \pm SD RF current and impedance were $0.67 \pm 0.2\text{A}$, and $45.8 \pm 6.5\Omega$, respectively. The mean \pm SD of the short-axis diameters of ablation zones on CE T1WI was 20.7 ± 3.5 mm in acute lesions and 17.7 ± 5.4 mm in chronic lesions. Significant increase ($p=0.02$) in blood pressure was noted during ablation. Insignificant increases ($p>0.05$) in epinephrine, norepinephrine, glucose and ACTH levels and insignificant decrease ($p>0.05$) in cortisol level were recorded during adrenal ablations. 2 outliers with marked rise in epinephrine level were noted- one corresponded with the highest blood pressure increase.

Conclusion: MRI-guided intervention within the new open bore scanner combines accessibility with the full advantages of a high field system including significantly high SNR images obtainable within efficient time frames. Percutaneous RFA of the adrenal glands was successfully performed under exclusive MRI guidance and monitoring. Targeting an adrenal neoplasm in a human subject is expected to be a simpler task compared to the thin linear porcine glands attempted in the current study. The MR imaging appearance of adrenal ablation zones is generally similar to the reported appearance of RF induced ablations in other organs and tissues. The herein reported significant increase in blood pressure during ablation explains the sporadic prior reports (1) of hypertensive crises during adrenal interventions. A better understanding of the underlying blood chemistry changes awaits further animal experiments to achieve enough statistical power.

References: (1) J Vasc Interv Radiol. 2006;17(3):573-5.

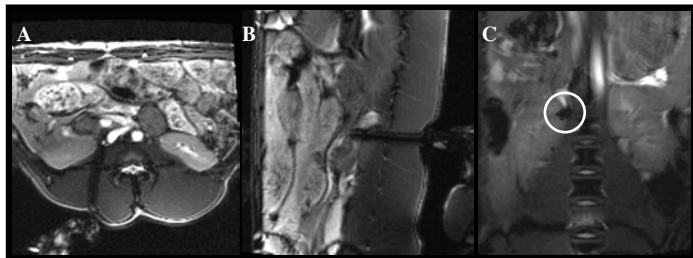


Fig. 1: Real-time triplane guidance of the RF electrode under True-FISP

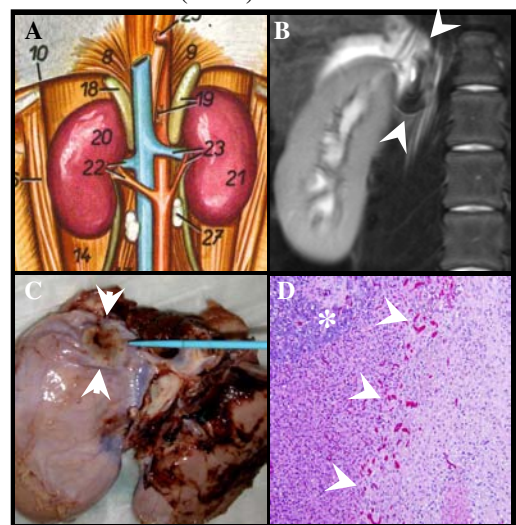


Fig.2: (A) The adrenal glands (18 & 19) in porcine models are thin linear structures along the medial aspect of the upper kidney poles (Popesco P, Atlas of Topographical Anatomy of the Domestic Animals, Vol 1, 5th edition, 1986) (B) Coronal gadolinium-enhanced TSE T2WI following ablation demonstrating central hypointense zone of coagulation necrosis surrounded by bright rim (arrows) (C&D) Corresponding gross and histological pathology show the area of necrosis with marginal hyperemia (arrowheads). The asterisk